

Optimal Reduced-order Modeling of Bipedal Locomotion

Yu-Ming Chen¹ and Michael Posa¹

Abstract—State-of-the-art approaches to legged locomotion are widely dependent on the use of models like the linear inverted pendulum (LIP) and the spring-loaded inverted pendulum (SLIP), popular because their simplicity enables a wide array of tools for planning, control, and analysis. However, they inevitably limit the ability to execute complex tasks or agile maneuvers. In this work, we aim to automatically synthesize models that remain low-dimensional but retain the capabilities of the high-dimensional system. For example, if one were to restore a small degree of complexity to LIP, SLIP, or a similar model, our approach discovers the form of that additional complexity which optimizes performance. In this paper, we define a class of reduced-order models and provide an algorithm for optimization within this class. To demonstrate our method, we optimize models for walking at a range of speeds and ground inclines, for both a five-link model and the Cassie bipedal robot.

I. INTRODUCTION

Modern legged robots, like the Agility Robotics Cassie, have many degrees of freedom, tens or more actuators and may have passive dynamic elements such as springs and dampers. To manage this complexity, and simplify the process of planning and control design, the community has embraced the use of reduced-order models. Particularly popular are the linear inverted pendulum (LIP) [1], [2], the spring-loaded inverted pendulum (SLIP) [3], and various permutations. The LIP has a long history as a predominant approach in robot walking, and formed the basis of many approaches taken during the DARPA robotics challenge [4], [5], [6]. The SLIP is widely used to explain energy efficient running [7], [8], [9], [10]. These models have been empirically shown to capture the dominant dynamics of the robots in particular tasks, and their simplicity enables solutions to the challenging problems of control and planning design. For example, many of locomotion planning problems can be solved in realtime with the low-dimensional models [11].

The downside, however, is that by forcing robots to act like a low-degree-of-freedom model, these approaches restrict the motion of complex robots and necessarily sacrifices performance. This can result in energetically inefficient motion, or fail to extend to wide range of tasks. For example, the LIP greatly restricts both efficiency and stride length. These limitations have long been acknowledged by the community, resulting in a wide array of extensions that universally rely on human intuition, and are generally in the form of mechanical components (a spring, a damper, a joint, a rigid body with inertia, etc) [12], [13], [14], [15], [16], [17], [18].

¹Yu-Ming Chen and Michael Posa are with the General Robotics, Automation, Sensing and Perception (GRASP) Laboratory, University of Pennsylvania, Philadelphia, PA 19104, USA {ymchen, posa}@seas.upenn.edu

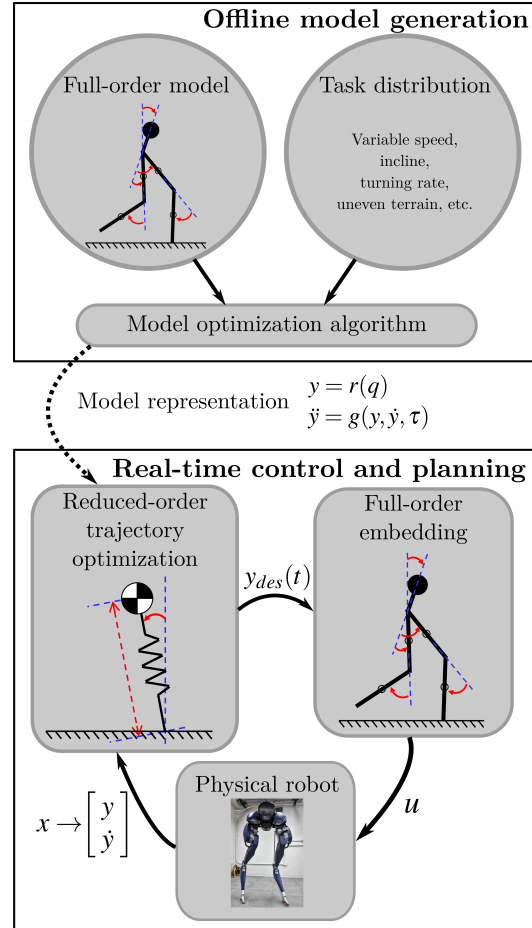


Fig. 1: An outline of the synthesis and deployment of optimal reduced-order models. Offline, given a full-order model and a distribution of tasks, we optimize a new model that is effective over the task space. Online, we generate new plans for the reduced-order model and track these trajectories on the true, full-order system.

The ad hoc nature of these extensions demonstrates that the community implicitly admits both that the simplest models are insufficient, and that it is not known which extensions are most beneficial. Additionally, it has been shown that not all model extensions improve the performance of robots much. For example, allowing center of mass height to vary provides limited aid in the task of balancing [19], [20].

The primary contribution of this paper is an optimization algorithm to automatically synthesize new reduced order models, embedding high-performance capabilities within low-dimensional representations. Given a distribution of

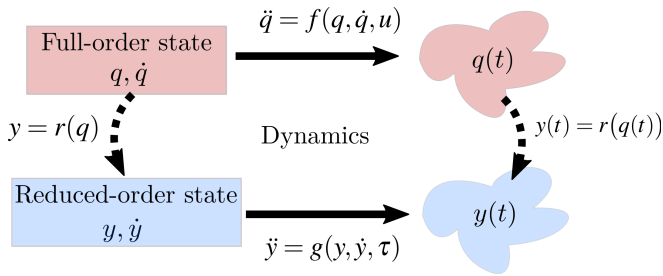


Fig. 2: Relationship of the full-order and reduced-order models. The generalized positions q and y satisfy the embedding function r for all time, and the evolution of the velocities \dot{q} and \dot{y} respects the dynamics f and g , respectively.

tasks, and a nominal full-order model, we propose a bilevel optimization of stochastic gradient descent and trajectory optimization to search within a broad class of simple models.

II. BACKGROUND

A. Walking via simple models

A good simple model is a low-dimensional representation that captures much of the relevant dynamics while enabling effective control design, a concept closely related to that of templates and anchors [21], [22]. One observation, common to many approaches, lies in the relationship between foot placement, ground reaction forces, and the center of mass (COM). While focusing on the COM neglects the individual robot limbs, controlling the COM position has proven to be an excellent proxy for the stability of a walking robot. COM-based simple models include the LIP [1], [2], which restricts angular momentum and vertical motion, SLIP [3], hopping models [23], inverted pendulums [24], [25], [26], [27], [28], and others. Since these models are universally low-dimensional, they have enabled a variety of control synthesis and analysis techniques that would not otherwise be computationally tractable. For example, numerical methods have been successful at finding robust gaits and control designs [29], [30], [31], [32], and assessing stability [33]. A common approach, which we also adopt in this work, is to first plan motions of the reduced-order model, and then track this lower-dimensional trajectory with a technique like operational space control [34].

Despite their successes, many deficiencies have been found in these simplest models (e.g [35]). For example, by eliminating the use of angular momentum and prohibiting impacts, the LIP greatly reduces energy efficiency and limits speed and stride length. This has necessitated extensions (e.g. [16] and others), where all replace inverted pendulum abstractions with that of a more complex physical model.

B. Trajectory optimization

This paper will heavily leverage trajectory optimization within the inner loop of a bilevel optimization problem. We briefly review the area here, but the reader is encouraged to see [36] for a more complete description. Generally speaking, trajectory optimization is a process of finding state $x(t)$ and

input $u(t)$ that minimize some measure of cost h while satisfying a set of constraints C . Following the approach taken in prior work [37], [38], we explicitly optimize over state, input, and constraint (contact) forces $\lambda(t)$,

$$\begin{aligned} \min_{x(t), u(t), \lambda(t)} & \int_{t_0}^{t_f} h(x(t), u(t)) dt \\ \text{s.t.} & \dot{x}(t) = f(x(t), u(t), \lambda(t)), \\ & C(x(t), u(t), \lambda(t)) \leq 0, \end{aligned} \quad (1)$$

where f is the dynamics of the system, λ are the forces required to satisfy holonomic constraints, and t_0 and t_f are the initial and the final time respectively. Standard approaches discretize in time, formulating (1) as a finite-dimensional nonlinear programming problem. For the purposes of this paper, any such method would be appropriate; we use DIRCON [38] to address the closed kinematic chains present in the Cassie robot. DIRCON transcribes the infinite dimensional problem in (1) into a finite dimensional nonlinear problem

$$\begin{aligned} \min_w & \sum_{i=1}^{n-1} \frac{1}{2} (h(x_i, u_i) + h(x_{i+1}, u_{i+1})) \delta_k \\ \text{s.t.} & f_c(x_i, x_{i+1}, u_i, u_{i+1}, \lambda_i, \lambda_{i+1}, \delta_i, \alpha_i) = 0, \\ & \delta_i = 0, \quad i = 1, \dots, n-1 \\ & C(x_i, u_i, \lambda_i) \leq 0, \quad i = 1, \dots, n \end{aligned} \quad (2)$$

where n is the number of knot points, f_c is the collocation constraint for dynamics, and the decision variables are

$$w = [x_1, \dots, x_n, u_1, \dots, u_n, \lambda_1, \dots, \lambda_n, \delta_1, \dots, \delta_{n-1}, \alpha_1, \dots, \alpha_{n-1}]^T \in \mathbb{R}^{n_w}.$$

where δ_i 's are time intervals, and α_i 's are slack variables specific to DIRCON.

III. APPROACH

In this section, we first propose a concrete definition of reduced-order models, along with a notion of quality (or cost) for such models. We then introduce a bilevel optimization algorithm to optimize within our class of models.

A. Definition of reduced-order models

Let q and u be the generalized position and input of the full-order model, and let y and τ be the generalized position and input of the reduced-order model. We define a reduced-order model μ of dimension n_y by two things – an embedding function $r : q \mapsto y(q)$ and the second-order dynamics of the reduced-order model $g(y, \dot{y}, \tau)$.

$$\mu \triangleq (r, g), \quad (3)$$

with

$$\begin{aligned} y &= r(q), \\ \ddot{y} &= g(y, \dot{y}, \tau), \end{aligned} \quad (4)$$

where $\dim y < \dim q$ and $\dim \tau \leq \dim u$. As an example, to represent SLIP, r is the spring length and the spring angle with respect to the normal direction of ground, g is the spring-mass dynamics, and $\dim \tau = 0$ as SLIP is passive.

Fig. 2 shows the relationship between the two models. If we integrate the two models forward in time with their own dynamics, the resultant trajectories will still satisfy the embedding function r at any time in the future.

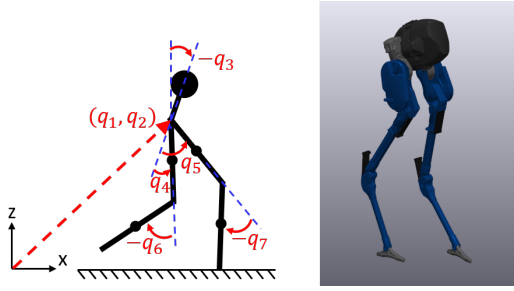


Fig. 3: Examples of full-order models. On the left is a five-link robot. On the right is the 3D Cassie biped, which has five actuators per leg.

loop (to trajectory optimization in the inner loop). That is, we sample a set of tasks from the distribution of Γ and optimize the averaged sample cost over the model parameters θ .

The full approach to (O) is outlined in Algorithm 1. Starting from an initial parameter seed θ_0 , N tasks are sampled, and the cost for each task is evaluated by solving the corresponding trajectory optimization problem (TO).

To compute each gradient $\nabla_{\theta} [\mathcal{J}_{\gamma_j}(\theta)]$, we adopt an approach based in sequential quadratic programming. We locally approximate (TO) with an equality-constrained quadratic program, only considering the active constraints. Let $\tilde{w}_{\gamma} = w - w_{\gamma}^*$ and $\tilde{\theta} = \theta - \theta^{(i)}$, where w_{γ}^* is the optimal solution of (TO), and $\theta^{(i)}$ is the parameter at the i -th iteration. The approximated quadratic program is

$$\begin{aligned} \mathcal{J}_{\gamma}(\theta) \approx \min_{\tilde{w}_{\gamma}} & \frac{1}{2} \tilde{w}_{\gamma}^T H_{\gamma} \tilde{w}_{\gamma} + b_{\gamma}^T \tilde{w}_{\gamma} + c_{\gamma} \\ \text{s.t.} & F_{\gamma} \tilde{w}_{\gamma} + G_{\gamma} \tilde{\theta} = 0 \end{aligned} \quad (8)$$

Using the KKT conditions, we can derive the following equation for the optimal solution

$$\begin{bmatrix} H_{\gamma} & F_{\gamma}^T \\ F_{\gamma} & 0 \end{bmatrix} \begin{bmatrix} \tilde{w}_{\gamma}^* \\ v_{\gamma}^* \end{bmatrix} = \begin{bmatrix} -b_{\gamma} \\ -G_{\gamma} \tilde{\theta} \end{bmatrix}, \quad (9)$$

where v_{γ}^* is the optimal dual solution. (9) can be further solved, with the solution rewritten as

$$\tilde{w}_{\gamma}^* = Q_{\gamma} \tilde{\theta} + p_{\gamma}, \quad (10)$$

for some $Q_{\gamma} \in \mathbb{R}^{n_w \times n_{\theta}}$ and $p_{\gamma} \in \mathbb{R}^{n_w}$. Since we approximate the original problem around w^* and $\theta^{(i)}$, we know that $\tilde{w}_{\gamma}^* = 0$ if $\tilde{\theta} = 0$; therefore, $p_{\gamma} = 0$. Substituting (10) into (8) and taking the gradient, we derive

$$\nabla_{\theta} [\mathcal{J}_{\gamma_j}(\theta)] \Big|_{\theta=\theta^{(i)}} = Q_{\gamma_j}^T b_{\gamma_j}. \quad (11)$$

The algorithm is deemed to have converged if the norm of the gradient falls below a specified threshold.

IV. EXAMPLES

We test our algorithm of model optimization with two robots: a five-link planar robot and the three dimensional Cassie biped (Fig. 3). For all examples, the motions of the optimized models are shown in the accompanying video. Examples were generated using the Drake software toolbox [41] and source code is freely available¹.

¹<https://github.com/DAIRLab/dairlib/tree/goldilocks-model-dev>

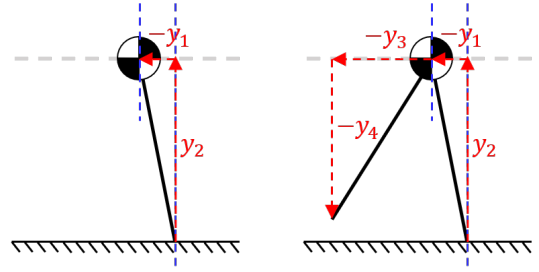


Fig. 4: Two initial reduced-order models with generalized positions. On the left is the standard LIP; on the right is an LIP with an actuated swing foot.

The planar robot consists of five links with non-zero mass and inertia, and four actuated joints with torque saturation. The thighs and shanks are of mass 2.5 kg and length 0.5 m. The weight of the torso is 10 kg and the length is 0.3 m. The robot has point feet, and the contacts between feet and ground are perfectly inelastic.

The Cassie has stiff rotational springs in the knees and ankles. Here, however, we simplify the model by treating these springs as infinitely stiff; this simplification is necessary for the coarse integration steps used in trajectory optimization, and has been used successfully with Cassie [42]. The legs also contain two four-bar linkages, which we model with a fixed-distance constraint and corresponding constraint force. There are five motors on each leg. Three located at the hip, one at the knee, and one at the toe.

The hybrid equations of motion of either robot are written

$$\begin{cases} \dot{x} = f(x, u), & x^- \notin S \\ x^+ = \Delta(x^-, \Lambda), & x^- \in S \end{cases} \quad (12)$$

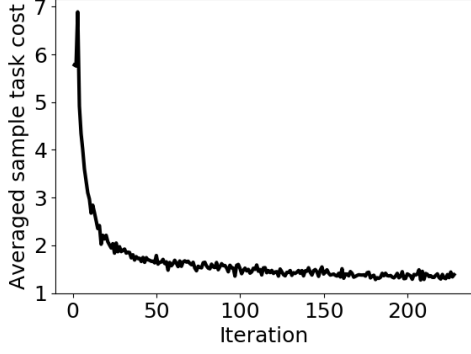
where x^- and x^+ are pre- and post-impact state, Λ is the impulse of swing foot touchdown, Δ is the discrete mapping of the touchdown event, and S is the surface in the state space where the event must occur.

We assume the robot walks with instantaneous change of support. That is, the robot transitions from right support to left support instantaneously, and vice versa. Therefore, the phase sequence cycles through a single support phase. For the examples here, we consider only half-gait periodic motion, and so include right-left leg alternation in the impact map Δ .

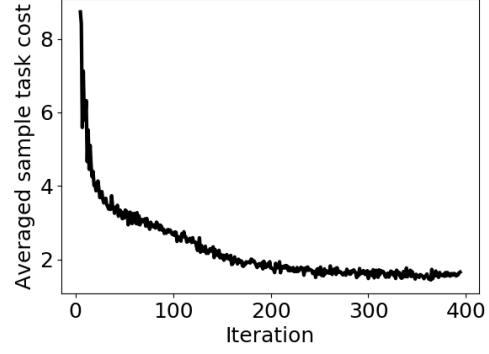
A. Initial reduced-order models

To demonstrate the algorithm, we optimize two models for each robot. The first is 2 dimensional, with 0 inputs, and the second is 4 dimensional with 2 inputs. We initialize the 2D model with an LIP and the 4D model with an LIP plus a point-mass swing foot (Fig. 4). The generalized positions y for both models are shown in Fig. 4. For reference, the equations of motion of the LIP with a point-mass swing foot are

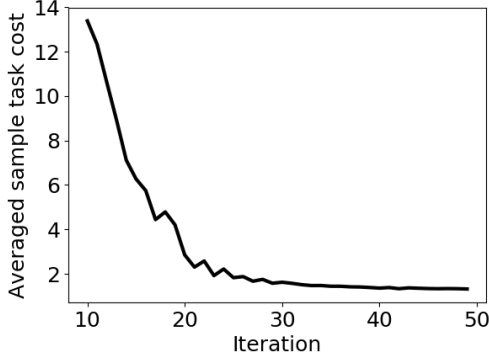
$$\ddot{y} = \begin{bmatrix} \ddot{y}_1 \\ \ddot{y}_2 \\ \ddot{y}_3 \\ \ddot{y}_4 \end{bmatrix} = \begin{bmatrix} c_g \cdot y_1/y_2 \\ 0 \\ 0 \\ 0 \end{bmatrix} + \begin{bmatrix} 0 & 0 \\ 0 & 0 \\ 1 & 0 \\ 0 & 1 \end{bmatrix} \begin{bmatrix} \tau_1 \\ \tau_2 \end{bmatrix}, \quad (13)$$



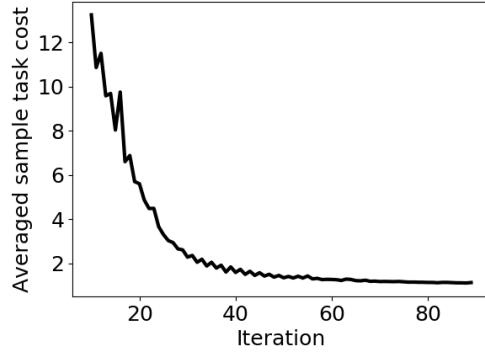
(a) 2D reduced-order model embedded in the five-link planar robot.



(b) 4D reduced-order model embedded in the five-link planar robot.



(c) 2D reduced-order model embedded in Cassie.



(d) 4D reduced-order model embedded in Cassie.

Fig. 5: The averaged cost of the sampled tasks over iterations. Costs are normalized by the cost associated with the full-order model (a lower bound on any reduced-order model).

where $c_g = 9.81 \text{ m/s}^2$ is the gravitational acceleration. For the LIP, the dynamics are given in the first two rows of (13).

B. Five-link planar robot

For the case of five-link robot, we have $q \in \mathbb{R}^7$, where the first 3 elements are the floating-base joint. Recall that the contact constraint with the ground is solved implicitly.

We choose a rich feature set ϕ_e that includes the COM position with respect to the stance foot, the swing foot position with respect to the center of mass, the hip position (q_1, q_2) , and all quadratic combinations of the elements in $\{1, \cos(q_3), \sin(q_3), \dots, \cos(q_7), \sin(q_7)\}$.

For the 2D model, the feature set ϕ_d includes $c_g \cdot y_1/y_2$, and all quadratic combinations of the elements in $\{1, y_1, y_2, \dot{y}_1, \dot{y}_2\}$. For the 4D model, the feature set ϕ_2 is constructed in a similar way. Note that these feature vectors were chosen to explicitly include elements of the LIP and the LIP with a swing foot, but also include a diverse set of additional terms. Initial parameters θ can be easily chosen to match the LIP-based initial models.

We chose Γ to include walking with different speeds between 0.27 and 0.54 m/s and on ground inclines between -0.08 and 0.08 radians. The cost h_γ is the sum of weighted norm of generalized velocity \dot{q} , input of the robot u and

input of the reduced-order model τ . We include τ in the cost to regularize the input to the reduced-order model, and to correlate it with cost on the original model.

Fig. 5a and 5b show results from optimization, where the empirical average cost decreases rapidly during the process. Note that the empirical average does not strictly decrease, as tasks are randomly sampled and are of varying difficulty. The optimized model is capable of expressing lower cost and more natural motion than the LIP, better leveraging the natural dynamics of the five-link model.

C. Cassie

For the 3D Cassie, the generalized position $q \in \mathbb{R}^{19}$ is 19 dimensional, and the first 7 elements are the floating-base joint (translation and rotation expressed via quaternion). The feature sets ϕ_e and ϕ_d are constructed in a similar way to that of the five-link robot example. We pick the task set Γ to be walking with different speeds between 0.25 and 0.75 m/s and on different ground inclines between -0.08 and 0.08 radians. For this example, to reduce runtime of the trajectory optimization subproblems, we chose a finite set of 9 tasks, evenly distributed in the task space.

Results, showing average cost per iteration, are shown in Fig. 5c and 5d. As with the simpler example, reduced-

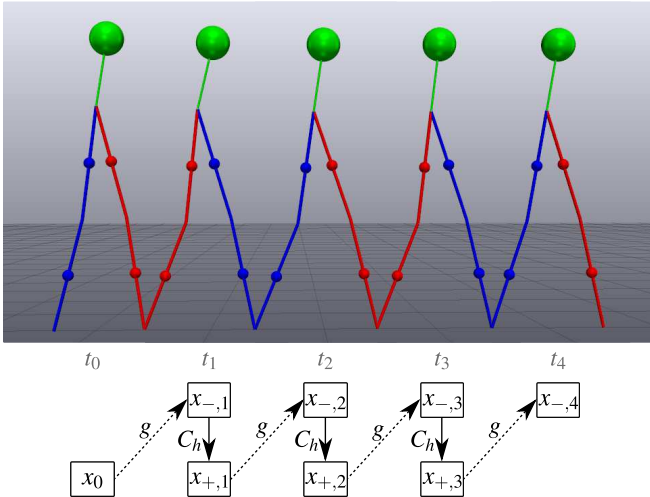


Fig. 6: Given a task of covering two meters in five steps, we rapidly plan a trajectory for the reduced-order model. The high-dimensional model is used to capture the hybrid event, at stepping, as illustrated in the cartoon.

order model optimization maintains model simplicity but dramatically improves performance. Furthermore, we note that the final, optimized model, unlike its classical counterpart, does not map easily to a simple, physical model. While this limits our ability to attach physical meaning to y and τ , we believe this to be a necessary sacrifice to improve performance beyond that of hand-designed approaches.

V. PLANNING WITH REDUCED-ORDER MODELS

As shown in Fig. 1, given an optimal model μ^* , we plan in the reduced-order space. As an example, we formulate a trajectory optimization problem to walk l meters in n_s strides. Since the reduced-order model only captures the continuous dynamics, and perfect embedding of a reduced-order hybrid model is often impossible, we mix the reduced-order model with the discrete dynamics from the full-order model. This approach results in a low-dimensional trajectory optimization problem, a search for $y_j(t)$ and $\tau_j(t)$, with additional decision variables $x_{-,j}, x_{+,j}$, representing the pre- and post-impact full-order states. The index $j = 1, \dots, n_s$ refers to the j th stride; note that the reduced-order model trajectories are necessarily hybrid. Where t_j 's are the impact times (ending the j th stride), additional constraints relate these full-order states to the impact mapping and the reduced order model,

$$\begin{aligned}
 y_j(t_j) &= r(q_{-,j}; \theta_e), & j &= 1, \dots, n_s - 1, \\
 y_{j+1}(t_j) &= r(q_{+,j}; \theta_e), & j &= 1, \dots, n_s - 1, \\
 \dot{y}_j(t_j) &= \frac{\partial r(q_{-,j}; \theta_e)}{\partial q_{-,j}} \dot{q}_{-,j}, & j &= 1, \dots, n_s - 1, \\
 \dot{y}_{j+1}(t_j) &= \frac{\partial r(q_{+,j}; \theta_e)}{\partial q_{+,j}} \dot{q}_{+,j}, & j &= 1, \dots, n_s - 1, \\
 0 &\geq C_{\text{hybrid}}(x_{-,j}, x_{+,j}, \Lambda_j), & j &= 1, \dots, n_s - 1.
 \end{aligned}$$

C_{hybrid} represents the hybrid guard S and the impact mapping Δ without left-right leg alternation. Costs are nominally ex-

pressed in terms of $[y^\top, \dot{y}^\top]^\top$ and τ , though the pre- and post-impact full-order states can also be used to represent goal locations. This formulation preserves an exact representation of the hybrid dynamics, but results in a significantly reduced optimization problem that can be used for real-time planning.

We tested the planning algorithm with the optimized 4D model embedded in the five-link robot. The distance l varies from 0.2 to 6 meters with stride numbers n_s between 1 to 10. To plan a single step, the average runtime was 110ms, on a computer with Intel i7-8750H processor, without optimizing code for efficiency. Similar code required minutes for the full-order model. Fig. 6 visualizes the pre-impact states in the case where the robot walks two meters with four strides, connected by the hybrid events and continuous low-dimensional trajectories $y_j(t)$. We were able to retrieve $q(t)$ from $y_j(t)$ through inverse kinematics, meaning that the optimal trajectories $y_j(t)$ are feasible for the robot. The resulting motion, shown in the accompanying video, looks smooth and is qualitatively more efficient than the gait that the original model (LIP with a foot) would generate.

This demonstrates that the mixed model planner greatly reduces planning speed, and that the optimized reduced-order models can be used to achieve tasks in full-order space.

VI. DISCUSSION

We present a novel method for automatically generating reduced-order models for legged locomotion, a step toward uncovering which aspects of the dynamics are necessary for tasks performance. This approach is demonstrated over an array of tasks on both a simple, planar robot and a 3D model of the Cassie. We also present an algorithm, suitable for real-time use, for planning reduced-order trajectories.

While there is no guarantee that the motions planned in Section V are feasible for the full model, we observe, empirically, that embeddings do seem to exist, and also note that classical models like LIP also provide no guarantees. One direction for future work, for both LIP and the optimized models, is to generate constraints for reduced-order planning that guarantee feasibility on the original system.

Other future work will continue to develop and deploy reduced-order models, with an immediate goal of tracking and executing the planned motions on the physical Cassie robot using operational space control (e.g. [34]). In Section V, we note that the planner must still use the full-order model for the discrete mapping; future work will explore optimization of hybrid reduced-order model. Since impact maps are fully autonomous, it is not possible to find a perfect, low-order reduction. This necessitates the need for approximate hybrid models, where we will leverage existing notions of hybrid distance [43]. Lastly, we would like to increase the tasks space and explore alternative function bases to evaluate the quality of different resulting models.

REFERENCES

- [1] S. Kajita and K. Tani, "Study of dynamic biped locomotion on rugged terrain-derivation and application of the linear inverted pendulum mode," vol. 2, pp. 1405–1411, IEEE International Conference on Robotics and Automation (ICRA), 1991.

- [2] S. Kajita, F. Kanehiro, K. Kaneko, K. Yokoi, and H. Hirukawa, "The 3D linear inverted pendulum mode: a simple modeling for a biped walking pattern generation," pp. 239–246, IEEE International Conference on Intelligent Robots and Systems (IROS), 2001.
- [3] R. Blickhan, "The spring-mass model for running and hopping," *Journal of biomechanics*, vol. 22, no. 11-12, pp. 1217–1227, 1989.
- [4] S. Feng, E. Whitman, X. Xinjilefu, and C. G. Atkeson, "Optimization-based Full Body Control for the DARPA Robotics Challenge," *Journal of Field Robotics*, vol. 32, no. 2, pp. 293–312, 2015.
- [5] T. Koolen, J. Smith, G. Thomas, S. Bertrand, J. Carff, N. Mertins, D. Stephen, P. Abeles, J. Engelsberger, S. McCrory, J. van Egmond, M. Griffioen, M. Floyd, S. Kobus, N. Manor, S. Alsheikh, D. Duran, L. Bunch, E. Morphis, L. Colasanto, K.-L. H. Hoang, B. Layton, P. Neuhaus, M. Johnson, and J. Pratt, "Summary of Team IHMC's Virtual Robotics Challenge Entry," in *Proceedings of the IEEE-RAS International Conference on Humanoid Robots*, (Atlanta, GA), oct 2013.
- [6] S. Kuindersma, R. Deits, M. Fallon, A. Valenzuela, H. Dai, F. Permenter, T. Koolen, P. Marion, and R. Tedrake, "Optimization-based locomotion planning, estimation, and control design for Atlas," *Autonomous Robots*, vol. 40, no. 3, pp. 429–455, 2016.
- [7] M. Hutter, C. D. Remy, M. A. Höpflinger, and R. Siegwart, "Slip running with an articulated robotic leg," in *2010 IEEE/RSJ International Conference on Intelligent Robots and Systems*, pp. 4934–4939, IEEE, 2010.
- [8] I. Poulakakis and J. W. Grizzle, "The spring loaded inverted pendulum as the hybrid zero dynamics of an asymmetric hopper," *IEEE Transactions on Automatic Control*, vol. 54, no. 8, pp. 1779–1793, 2009.
- [9] C. Hubicki, A. Abate, P. Clary, S. Rezazadeh, M. Jones, A. Peekema, J. Van Why, R. Domres, A. Wu, W. Martin, et al., "Walking and running with passive compliance," *IEEE ROBOTICS AND AUTOMATION MAGAZINE*, vol. 1, 2016.
- [10] W. C. Martin, A. Wu, and H. Geyer, "Experimental evaluation of deadbeat running on the atrias biped," *IEEE Robotics and Automation Letters*, vol. 2, no. 2, pp. 1085–1092, 2017.
- [11] T. Apgar, P. Clary, K. Green, A. Fern, and J. W. Hurst, "Fast online trajectory optimization for the bipedal robot cassie.," in *Robotics: Science and Systems*, 2018.
- [12] J. Pratt, P. Dilworth, and G. Pratt, "Virtual model control of a bipedal walking robot," in *Proceedings of International Conference on Robotics and Automation*, vol. 1, pp. 193–198, IEEE, 1997.
- [13] R. Sellaoui, O. Stasse, S. Kajita, K. Yokoi, and A. Kheddar, "Faster and smoother walking of humanoid hrp-2 with passive toe joints," in *2006 IEEE/RSJ International Conference on Intelligent Robots and Systems*, pp. 4909–4914, IEEE, 2006.
- [14] M. Hutter, C. D. Remy, M. A. Hoepflinger, and R. Siegwart, "Scarleth: Design and control of a planar running robot," in *2011 IEEE/RSJ International Conference on Intelligent Robots and Systems*, pp. 562–567, IEEE, 2011.
- [15] G. Garofalo, C. Ott, and A. Albu-Schäffer, "Walking control of fully actuated robots based on the bipedal slip model," in *2012 IEEE International Conference on Robotics and Automation*, pp. 1456–1463, IEEE, 2012.
- [16] S. Faraji and A. J. Ijspeert, "3lp: A linear 3d-walking model including torso and swing dynamics," *the international journal of robotics research*, vol. 36, no. 4, pp. 436–455, 2017.
- [17] T. Koolen, T. De Boer, J. Rebula, A. Goswami, and J. Pratt, "Capturability-based analysis and control of legged locomotion, part 1: Theory and application to three simple gait models," *The International Journal of Robotics Research*, vol. 31, no. 9, pp. 1094–1113, 2012.
- [18] T. Libby, A. M. Johnson, E. Chang-Siu, R. J. Full, and D. E. Koditschek, "Comparative design, scaling, and control of appendages for inertial reorientation," *IEEE Transactions on Robotics*, vol. 32, no. 6, pp. 1380–1398, 2016.
- [19] M. Posa, T. Koolen, and R. Tedrake, "Balancing and Step Recovery Capturability via Sums-of-Squares Optimization," in *Robotics: Science and Systems*, 2017.
- [20] T. Koolen, M. Posa, and R. Tedrake, "Balance control using center of mass height variation: limitations imposed by unilateral contact," in *Humanoid Robots (Humanoids), 2016 IEEE-RAS 16th International Conference on*, pp. 8–15, IEEE, 2016.
- [21] R. J. Full and D. E. Koditschek, "Templates and anchors: neuromechanical hypotheses of legged locomotion on land," *The Journal of Experimental Biology*, vol. 202, pp. 3325–3332, 1999.
- [22] U. Saranlı, M. Buehler, and D. E. Koditschek, "RHex: A Simple and Highly Mobile Hexapod Robot," *The International Journal of Robotics Research*, vol. 20, pp. 616–631, jul 2001.
- [23] M. H. Raibert, H. B. Brown, and M. Chepponis, "Experiments in Balance with a 3D One-Legged Hopping Machine," *The International Journal of Robotics Research*, vol. 3, pp. 75–92, jun 1984.
- [24] M. Garcia, A. Chatterjee, A. Ruina, and M. Coleman, "The Simplest Walking Model: Stability, Complexity, and Scaling," *Journal of Biomechanical Engineering*, vol. 120, p. 281, apr 1998.
- [25] A. L. Schwab and M. Wisse, "BASIN OF ATTRACTION OF THE SIMPLEST WALKING MODEL," in *ASME 2001 Design Engineering Technical Conferences and Computers and Information in Engineering Conference*, 2001.
- [26] R. D. Gregg, A. K. Tilton, S. Candido, T. Bretl, and M. W. Spong, "Control and planning of 3-D dynamic walking with asymptotically stable gait primitives," *IEEE Transactions on Robotics*, vol. 28, no. 6, pp. 1415–1423, 2012.
- [27] P. A. Bhounsule, J. Cortell, A. Grewal, B. Hendriksen, J. G. D. Karssen, C. Paul, and A. Ruina, "Low-bandwidth reflex-based control for lower power walking: 65 km on a single battery charge," *The International Journal of Robotics Research*, vol. 33, pp. 1305–1321, sep 2014.
- [28] A. Hereid, S. Kolathaya, M. S. Jones, J. Van Why, J. W. Hurst, and A. D. Ames, "Dynamic multi-domain bipedal walking with atrias through SLIP based human-inspired control," in *Proceedings of the 17th international conference on Hybrid systems: computation and control - HSCC '14*, (New York, New York, USA), pp. 263–272, ACM Press, 2014.
- [29] K. Byl and R. Tedrake, "Metastable Walking Machines," *The International Journal of Robotics Research*, vol. 28, pp. 1040–1064, aug 2009.
- [30] C. Oguz Saglam and K. Byl, "Robust Policies via Meshing for Metastable Rough Terrain Walking," in *Robotics: Science and Systems*, 2014.
- [31] M. Kelly and A. Ruina, "Non-linear robust control for inverted-pendulum 2D walking," in *2015 IEEE International Conference on Robotics and Automation (ICRA)*, pp. 4353–4358, IEEE, may 2015.
- [32] T. Koolen, T. de Boer, J. Rebula, A. Goswami, and J. Pratt, "Capturability-based analysis and control of legged locomotion, Part 1: Theory and application to three simple gait models," *The International Journal of Robotics Research*, vol. 31, no. 9, pp. 1094–1113, 2012.
- [33] J. Pratt, J. Carff, S. Drakunov, and A. Goswami, "Capture point: A step toward humanoid push recovery," in *2006 6th IEEE-RAS international conference on humanoid robots*, pp. 200–207, IEEE, 2006.
- [34] P. M. Wensing and D. E. Orin, "Generation of dynamic humanoid behaviors through task-space control with conic optimization," in *2013 IEEE International Conference on Robotics and Automation*, pp. 3103–3109, IEEE, may 2013.
- [35] T. Suzuki and K. Ohnishi, "Trajectory Planning of Biped Robot with Two Kinds of Inverted Pendulums," in *2006 12th International Power Electronics and Motion Control Conference*, pp. 396–401, IEEE, aug 2006.
- [36] J. T. Betts, *Practical Methods for Optimal Control Using Nonlinear Programming*. SIAM Advances in Design and Control, Society for Industrial and Applied Mathematics, 2001.
- [37] M. Posa, C. Cantu, and R. Tedrake, "A Direct Method for Trajectory Optimization of Rigid Bodies Through Contact," *The International Journal of Robotics Research*, vol. 33, pp. 69–81, jan 2013.
- [38] M. Posa, S. Kuindersma, and R. Tedrake, "Optimization and stabilization of trajectories for constrained dynamical systems," in *2016 IEEE International Conference on Robotics and Automation*, vol. 2016-June, (Stockholm, Sweden), pp. 1366–1373, may 2016.
- [39] P. E. Gill, W. Murray, and M. A. Saunders, "{SNOPT}: An {SQP} Algorithm for Large-Scale Constrained Optimization," *SIAM Review*, vol. 47, no. 1, pp. 99–131, 2005.
- [40] C. R. Hargraves and S. W. Paris, "Direct Trajectory Optimization using Nonlinear Programming and Collocation," *J Guidance*, vol. 10, no. 4, pp. 338–342, 1987.
- [41] R. Tedrake and the Drake Team Development, "Drake: A planning, control, and analysis toolbox for nonlinear dynamical systems," 2016.
- [42] A. Hereid, O. Harib, R. Hartley, Y. Gong, and J. W. Grizzle, "Rapid bipedal gait design using c-frost with illustration on a cassie-series robot," *arXiv preprint arXiv:1807.06614*, 2018.
- [43] S. A. Burden, H. Gonzalez, R. Vasudevan, R. Bajcsy, and S. S. Sastry,

"Metrization and Simulation of Controlled Hybrid Systems," *IEEE Transactions on Automatic Control*, vol. 60, pp. 2307–2320, sep 2015.